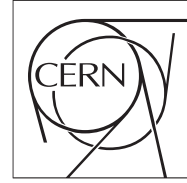**The Compact Muon Solenoid Experiment**

CMS Note

Mailing address: CMS CERN, CH-1211 GENEVA 23, Switzerland

June 20, 2011

A Search For New Physics in Z + Jets + MET using MET Templates

D. Barge, C. Campagnari, P. Kalavase, D. Kovalskyi, V. Krutelyov, J. Ribnik

University of California, Santa Barbara, USA

W. Andrews, G. Cerati, D. Evans, F. Golf, I. MacNeill, S. Padhi, Y. Tu, F. Würthwein, A. Yagil, J. Yoo

University of California, San Diego, USA

L. Bauerdick, I. Bloch, K. Burkett, I. Fisk, Y. Gao, O. Gutsche, B. Hooberman, S. Jindariani, J. Linacre

Fermi National Accelerator Laboratory, Batavia, Illinois, USA

Abstract

We search for new physics in the dilepton final state of Z plus two or more jets plus missing transverse energy (MET) in the $\sqrt{s} = 7$ TeV data in 2011 (204 pb^{-1}). The Z boson is reconstructed in its decay to e^+e^- or $\mu^+\mu^-$, and the search regions are defined as MET ≥ 100 GeV (loose signal region) and MET ≥ 200 GeV (tight signal region). We use data driven techniques to predict the standard model background in these search regions. Contributions from Drell-Yan production combined with detector mis-measurements that produce fake MET are modeled via MET templates. Top pair production background, as well as other backgrounds for which the lepton flavors are uncorrelated, are modeled via $e^\pm \mu^\mp$ subtraction.

Contents

15 Conclusion   **23**

A Triggers   **27**

B MET Templates from Photon Sample   **27**

1 Introduction

In this note we describe a search for new physics in the 2011 opposite sign isolated dilepton sample (ee, $e\mu$, and $\mu\mu$). The main sources of high p_T isolated dileptons at CMS are Drell Yan and $t\bar{t}$. Here we concentrate on dileptons with invariant mass consistent with $Z \to ee$ and $Z \to \mu\mu$. A separate search for new physics in the non-Z sample is described in [1].

We search for new physics in the final state of Z plus two or more jets plus missing transverse energy (MET). We reconstruct the Z boson in its decay to e^+e^- or $\mu^+\mu^-$. Our search regions are defined as MET $\geq$ 100 GeV (loose signal region) and MET $\geq$ 200 GeV (tight signal region), and two or more jets. We use data driven techniques to predict the standard model background in these search regions. Contributions from Drell-Yan production combined with detector mis-measurements that produce fake MET are modeled via MET templates based on photon plus jets or QCD events. Top pair production backgrounds, as well as other backgrounds for which the lepton flavors are uncorrelated such as WW and DY$\to \tau\tau$, are modeled via $e^{\pm}\mu^{\mp}$ subtraction.

As leptonically decaying Z bosons are a signature that has very little background, they provide a clean final state in which to search for new physics. Because new physics is expected to be connected to the Standard Model Electroweak sector, it is likely that new particles will couple to W and Z bosons. For example, in mSUGRA, low $M_{1/2}$ can lead to a significant branching fraction for $\chi_2^0 \to Z\chi_1^0$. In addition, we are motivated by the existence of dark matter to search for new physics with MET. Enhanced MET is a feature of many new physics scenarios, and R-parity conserving SUSY again provides a popular example. The main challenge of this search is therefore to understand the tail of the fake MET distribution in Z plus jets events.

The basic idea of the MET template method [2][3] is to measure the MET distribution in data in a control sample which has no true MET and a similar topology to the signal events. Templates can be derived from either a QCD sample (as was done in the original implementation) or a photon plus jets sample. In both cases, the instrumental MET is dominated by mismeasurements of the hadronic system, and can be classified by the number of jets in the event and the scalar sum of their transverse momenta. The prediction is made such that the jet system in the control sample is similar to that of the signal sample. By using two independent control samples–QCD and photon plus jets–we are able to illustrate the robustness of the MET templates method and to cross check the data driven background prediction.

This note is organized as follows. In sections 2 and 3.1 we descibe the datasets and triggers used, followed by the detailed object definitions (electrons, muons, photons, jets, MET) and event selections in sections 3.2 through 3.6. We define a preselection and compare data vs. MC yields passing this preselection in Section 4. We then define the signal regions and show the number of observed events and MC expected yields in Section 5. Section 6 introduces the MET template method and discusses its derivation in some detail and is followed by a demonstration in Section 7 that the method works in Monte Carlo. Section 8 introduces the top background estimate based on opposite flavor subtraction, and contributions from other backgrounds are discussed in Section 9. Section 10 shows the results for applying these methods in data. We analyze the systematic uncertainties in the background prediction in Section 11 and proceed to calculate an upper limit on the non-SM contributions to our signal regions in Section 12. Finally, in Section 14 we calculate upper limits on the quantity $\sigma \times BF \times A$, assuming efficiencies and uncertainties from sample benchmark SUSY processes.

2 Datasets

2.1 Datasets

We use the May 10 ReReco data for both leptons and photons.

For selecting the dilepton sample, the following datasets are used (the pythia DY samples are used only for generator level Z mass values less than 50 to avoid overlap with the madgraph DYJets sample):

- Data

    - /DoubleElectron/Run2011A-May10ReReco-v1/AOD

    - /DoubleMu/Run2011A-May10ReReco-v1/AOD

    - /MuEG/Run2011A-May10ReReco-v1/AOD

- Monte Carlo

    - /DYJetsToLL_TuneD6T_M-50_7TeV-madgraph-tauola/Spring11-PU_S1_START311_V1G1-v1/AODSI
    - /TTJets_TuneZ2_7TeV-madgraph-tauola/Spring11-PU_S1_START311_V1G1-v1/AODSIM
    - /WJetsToLNu_TuneZ2_7TeV-madgraph-tauola/Spring11-PU_S1_START311_V1G1-v1/AODSIM
    - /WWTo2L2Nu_TuneZ2_7TeV-pythia6/Spring11-PU_S1_START311_V1G1-v1/AODSIM
    - /WZtoAnything_TuneZ2_7TeV-pythia6-tauola/Spring11-PU_S1_START311_V1G1-v1/AODSIM
    - /ZZtoAnything_TuneZ2_7TeV-pythia6-tauola/Spring11-PU_S1_START311_V1G1-v1/AODSIM
    - /TToBLNu_TuneZ2_s-channel_7TeV-madgraph/Spring11-PU_S1_START311_V1G1-v1/AODSIM
    - /TToBLNu_TuneZ2_t-channel_7TeV-madgraph/Spring11-PU_S1_START311_V1G1-v1/AODSIM
    - /TToBLNu_TuneZ2_tW-channel_7TeV-madgraph/Spring11-PU_S1_START311_V1G1-v1/AODSIM
    - Pythia samples:
    - /DYToEE_M-20_CT10_TuneZ2_7TeV-powheg-pythia/Spring11-PU_S1_START311_V1G1-v1/AODSIM
    - /DYToMuMu_M-20_CT10_TuneZ2_7TeV-powheg-pythia/Spring11-PU_S1_START311_V1G1-v1/AODSI
    - /DYToTauTau_M-20_CT10_TuneZ2_7TeV-powheg-pythia-tauola/Spring11-PU_S1_START311_V1G1
    - /DYToEE_M-10To20_TuneZ2_7TeV-pythia6/Spring11-PU_S1_START311_V1G1-v1/AODSIM
    - /DYToMuMu_M-10To20_TuneZ2_7TeV-pythia6/Spring11-PU_S1_START311_V1G1-v1/AODSIM

For the creation of photon templates, we use:

- /Photon/Run2011A-May10ReReco-v1/AOD

The integrated luminosity used corresponds to 204 pb^{-1}, and the JSON used is the official May 10 ReReco JSON:
Cert_160404-163869_7TeV_May10ReReco_Collisions11_JSON.txt

3 Selection

3.1 Triggers

For data, we use a cocktail of unprescaled double lepton triggers. An event in the ee final state is required to pass at least one double electron trigger, a $\mu\mu$ event is required to pass at least one double muon trigger, while an $e\mu$ event is required to pass at least one $e - \mu$ cross trigger. $e\mu$ events are retained in a control sample used to estimate the ttbar contribution as described in Section 8.

The list of triggers used for selecting dilepton events can be found in Appendix A.1 for which the approximate efficiencies are 90% ($\mu\mu$), 95% ($e\mu$), 100% (ee).

Triggers used for creation of photon templates are listed in Section 6.

3.2 Event Selections

These event selections are implemented following the recommendation of PVT.

- If at least 10 tracks are present, at least 25% of them must be high purity.

- At least one primary vertex which passes the following selections is required:

    - Not fake
    - At least 5 degrees of freedom
    - $\rho < 2$ cm
    - $|z| < 24$ cm

5

3.3 Lepton Selection

Because Z $\rightarrow l^+l^-$ (where l is an electron or muon) is a final state with very little background after a Z mass requirement is applied to the leptons, we restrict ourselves to events in which the Z boson decays to electrons or muons only. Therefore two same flavor, opposite sign leptons passing the ID described below are required in each event.

- $p_T > 20$ GeV

- Opposite sign, same flavor ($e^\pm\mu^\mp$ events are retained in a control sample used to estimate the ttbar contribution)

- Dilepton invariant mass is consistent with the Z mass: between 81 and 101 GeV

- Electron ID

  - $|\eta| < 2.5$
  - VBTF 90 ID from the Egamma group[6], tightened to match HLT requirements CaloIdT+TrkIdVL which includes: [7]
    * H/E < 0.1 (0.075), $\sigma_{i\eta i\eta} < 0.011$ (0.031) in barrel (endcap)
    * d$\eta < 0.01$ (0.01), d$\phi < 0.15$ (0.1) in barrel (endcap)
  - $|d_0| < 0.04$ (with respect to the first DA primary vertex)
  - $|d_z| < 1.0$ (with respect to the first DA primary vertex)
  - Isolation: The sum of the p_T of tracks and the transverse energy in both calorimeters in a cone of $dR = 0.3$ divided by the p_T of the electron is required to be less than 0.15. In the barrel only, a pedestal of 1 GeV is subtracted from the ECAL energy.
  - No muon is allowed to be within $dR < 0.1$ of the electron
  - No more than one missing inner tracker hit [8]
  - In order to reject electrons from conversions, we veto electrons with a reconstructed conversion vertex [9]
  - Supercluster $E_T > 10$ GeV

- Muon ID

  - Muon $|\eta| < 2.4$
  - Muon global fit is required to have χ^2 divided by number of degrees of freedom less than 10
  - Required to be both global and tracker
  - Silicon track is required to have at least 11 hits
  - The ECAL energy in the calorimeter tower traversed by the muon cannot exceed 4 GeV
  - The HCAL energy in the calorimeter tower traversed by the muon cannot exceed 6 GeV
  - Must have at least one stand-alone hit
  - $|d_0| < 0.02$ (with respect to the first DA primary vertex)
  - $|d_z| < 1.0$ (with respect to the first DA primary vertex)
  - Relative transverse momentum error of silicon track used for muon fit is $\delta(p_T)/p_T < 0.1$
  - The muon is required to be a PF muon whose p_T is no more than 1 GeV different than the reco muon (to ensure consistency with PF MET)
  - The same isolation requirement is applied as in the electron case (but no pedestal is subtracted from the ECAL energy).

- Dilepton Selection

  - If more than 1 pair of leptons passing the above selection is present in the event, choose the pair with mass closest to M_Z. These leptons are referred to as the Z hypothesis leptons.

6

3.4 Photons

As will be explained later, it is not essential that we select real photons. What is needed are jets that are predominantly electromagnetic, well measured in the ECAL, and hence less likely to contribute to fake MET. We select "photons" with:

- $p_T > 22$ GeV

- $|\eta| < 2$

- $H/E < 0.1$

- There must be a pfjet of $p_T > 10$ GeV matched to the photon within $dR < 0.3$. The matched jet is required to have a neutral electromagnetic energy fraction of at least 70% (see section 7).

- We require that the pfjet p_T matched to the photon satisfy (pfjet p_T - photon p_T) > -5 GeV. This removes a few rare cases in which "overcleaning" of a pfjet generated fake MET.

- We also match photons to calojets and require (calojet p_T - photon p_T) > -5 GeV (the same requirement used for pfjets). This is to remove other rare cases in which fake energy is added to the photon object but not the calojet.

- We reject photons which have an electron of at least $p_T > 10$ GeV in order to reject conversions from electrons from W decays which are accompanied by real MET.

3.5 MET

We use pfMET, henceforth referred to simply as "MET."

3.6 Jets

- PF jets

- $|\eta| < 3.0$

- Passes loose pfjet ID

- L2L3 corrected

- L1Fastjet corrected to account for pile up

- $p_T > 30$ GeV for Njet counting, $p_T > 15$ GeV for sum jet p_T counting

- For the creation of photon templates, the jet matched to the photon passing the photon selection described above is vetoed

- For the dilepton sample, jets are vetoed if they are within $dR < 0.4$ from any lepton $p_T > 20$ GeV passing analysis selection

4 Preselection yields

Based on the event and trigger selections described in Section 3, we define a preselection as follows:

- Number of jets ≥ 2

- Same flavor dileptons (opposite flavor yields will be shown since they are used in data for $t\bar{t}$ background estimation)

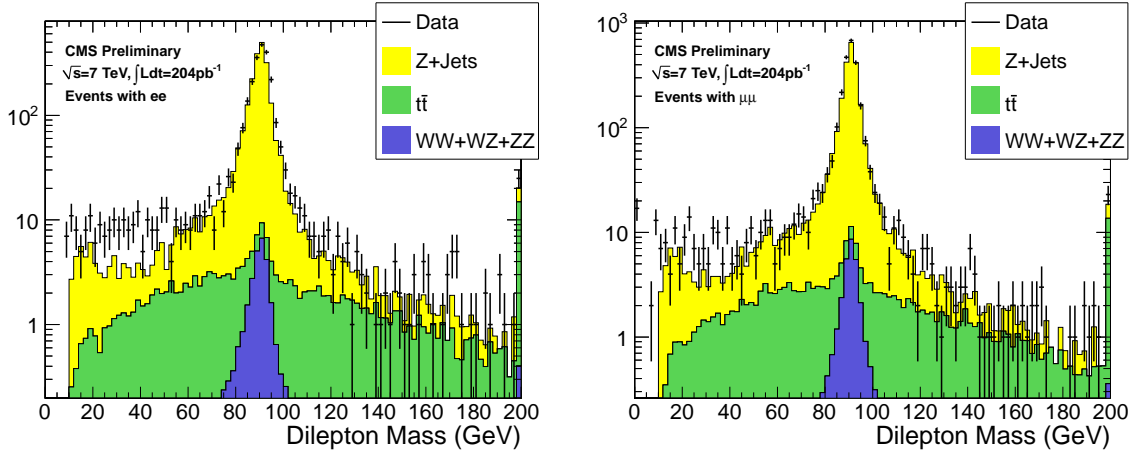- Dilepton mass within 10 GeV of the Z mass

Figure 1: Dilepton mass distribution for events passing the pre-selection for 204 pb^{-1} in the ee (left) and $\mu\mu$ (right) final states. Backgrounds from single top and W+jets are omitted since they are negligible.

The resulting dilepton mass spectra for the ee and $\mu\mu$ final states are shown in Figure 1.

The data yields and the MC predictions are given in Table 1.

The MC yields are normalized to 204 pb^{-1} using the cross-sections from Reference [10] assuming 100% trigger efficiency . As anticipated, the MC predicts that the preselection is dominated by Z+jets in the same-flavor case and by $t\bar{t}$ in the opposite-flavor case. The data yield is in reasonable agreement with the predictions for the ee, $\mu\mu$ and $e\mu$ channels. We also show the LO yields for the LM4 and LM8 processes, which are benchmark SUSY processes in which Z bosons are produced via cascade decays of SUSY particles.

Table 1: Data and Monte Carlo yields for the preselection for 204 pb^{-1}. The NLO yields for the SUSY benchmark processes LM4 and LM8 are also shown.

Sample	ee	$\mu\mu$	$e\mu$	tot
Z+Jets	1840.566 ± 21.213	2088.019 ± 22.592	1.467 ± 0.599	3930.052 ± 30.996
$t\bar{t}$	24.515 ± 0.860	25.965 ± 0.885	51.295 ± 1.244	101.775 ± 1.753
WJets	0.852 ± 0.603	0.000 ± 0.000	0.426 ± 0.426	1.278 ± 0.738
WW	0.217 ± 0.043	0.442 ± 0.061	0.593 ± 0.070	1.252 ± 0.102
WZ	13.947 ± 0.157	16.001 ± 0.168	0.111 ± 0.014	30.059 ± 0.230
ZZ	10.005 ± 0.076	11.364 ± 0.082	0.022 ± 0.004	21.391 ± 0.112
Single Top	0.725 ± 0.057	0.778 ± 0.059	1.694 ± 0.088	3.196 ± 0.120
Total MC	1890.827 ± 21.240	2142.569 ± 22.610	55.607 ± 1.450	4089.003 ± 31.056
Data	2051	2277	66	4394
LM4	2.027 ± 0.060	2.175 ± 0.062	0.291 ± 0.023	4.493 ± 0.089
LM8	0.889 ± 0.025	1.004 ± 0.026	0.273 ± 0.014	2.167 ± 0.038

5 Definition of the signal regions

We define signal regions to look for possible new physics contributions by adding the requirement of large MET to the preselection. Our choice of MET requirements to define the signal regions is driven by the MET distributions expected from Z and $t\bar{t}$ MC with the preselection applied, as shown in Fig. 2. The equivalent luminosity of the Z MC is approximately 834 pb^{-1}, and that of the $t\bar{t}$ sample is approximately 6.8 fb^{-1}.

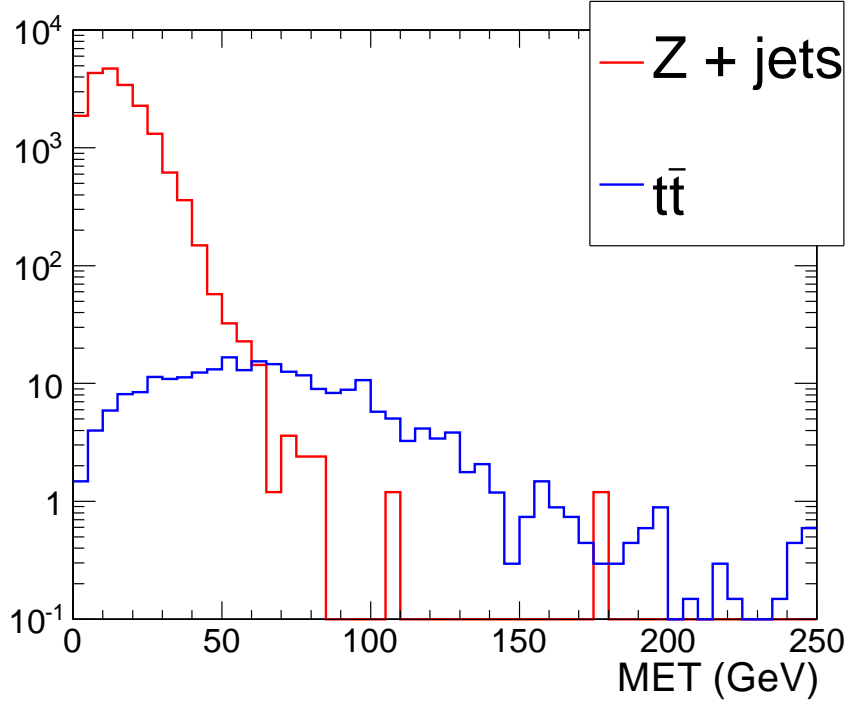We define two signal regions for our search:

- MET > 100GeV (loose signal region):

Figure 2: Distributions of MET in Z and $t\bar{t}$ MC normalized to 1 fb^{-1}.

In this region of MET there is a small contribution from the tail of the MET distribution in Z plus jets events. The bulk of the events in this region are from $t\bar{t}$ events where the leptons happen to be in the Z mass window.

The MC and data yields for this signal region are given in Table 2 and the dilepton mass distributions are shown in Fig. 3.

- MET > 200GeV (tight signal region): This signal region was selected by picking a region where the SM expectation is very low. At this kinematical region the dominant background contribution is expected to be from $t\bar{t}$.

The MC and data yields for this signal region are given in Table 3.

In the two signal regions above, the dominant background is $t\bar{t}$. However, it is still essential to have a data driven estimation of the Z contribution in the signal regions to demonstrate that we understand our background composition (see section 6). This is important both in case when an excess is observed or when placing a limit on new physics.

To estimate the $t\bar{t}$ background we will use the opposite flavor subtraction described in Section 8.

6 Modeling Instrumental MET using MET Templates

6.1 Introduction

The premise of this data driven technique is that MET in Z plus jets events is produced by the hadronic recoil system and *not* by the leptons making up the Z . Therefore, the basic idea of the MET template method is to measure the MET distribution in a control sample which has no true MET and the same general attributes regarding fake MET as in Z plus jets events. The original implementation of the template method used QCD dijet and multijet events to model the instrumental MET in lepton plus jets events. In this note, we use seperately templates derived from QCD events and photon plus jets events. We therefore have two independent control samples which each provide a separate prediction for the MET in the Z plus jets sample. This gives us extra confidence that the method is not very sensitive to the composition of the control sample.
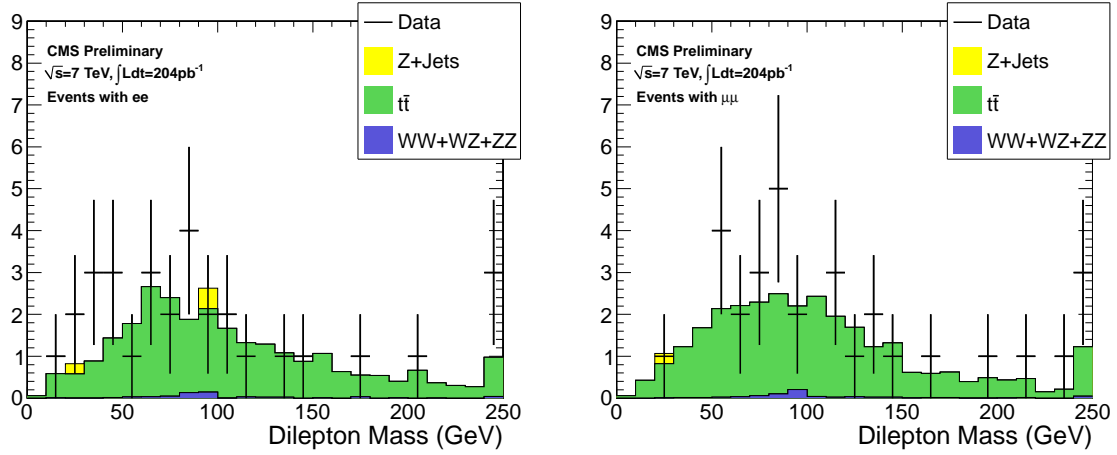
Figure 3: Dilepton mass distribution for events passing the pre-selection and MET > 100 GeV for 204 pb^{-1} in the ee (left) and $\mu\mu$ (right) final states. Backgrounds from single top and W+jets are omitted since they are negligible.

Table 2: Data and Monte Carlo yields for the loose signal region MET > 100 GeV for 204 pb^{-1}.

Sample	ee	$\mu\mu$	$e\mu$	tot
Z+Jets	0.489 ± 0.346	0.000 ± 0.000	0.000 ± 0.000	0.489 ± 0.346
$t\bar{t}$	3.714 ± 0.335	4.317 ± 0.361	8.454 ± 0.505	16.485 ± 0.705
WJets	0.000 ± 0.000	0.000 ± 0.000	0.000 ± 0.000	0.000 ± 0.000
WW	0.025 ± 0.014	0.058 ± 0.022	0.100 ± 0.029	0.184 ± 0.039
WZ	0.155 ± 0.017	0.144 ± 0.016	0.004 ± 0.002	0.303 ± 0.023
ZZ	0.088 ± 0.007	0.096 ± 0.007	0.000 ± 0.000	0.184 ± 0.010
Single Top	0.102 ± 0.021	0.133 ± 0.024	0.256 ± 0.034	0.490 ± 0.047
Total MC	4.572 ± 0.482	4.749 ± 0.363	8.814 ± 0.507	18.134 ± 0.788
Data	7	7	12	26
LM4	1.522 ± 0.052	1.603 ± 0.053	0.232 ± 0.020	3.356 ± 0.077
LM8	0.597 ± 0.020	0.686 ± 0.022	0.219 ± 0.012	1.502 ± 0.032

In selecting both QCD and photon plus jets events, the jet selection from section 3.6 is used. For selection photon-like objects, the very loose photon selection described in section 3.4 is used. It is not essential for the photon sample to have high purity. For our purposes, selecting jets with predominantly electromagnetic energy deposition in a good fiducial volume suffices to ensure that they are well measured and do not contribute to fake MET.

The MET in these events is dominated by mismeasurements of the hadronic system. To account for kinematic differences between the hadronic systems in the control vs. signal samples, we measure the MET distributions in the control sample in bins of the number of jets and the scalar sum of jet p_T . The Njet binning used is 2 jets and ≥ 3 jets. The sum jet p_T binning is defined by the boundaries 60, 90, 120, 150, 250, 5000 GeV. These MET distributions normalized to unity form the MET templates.

The prediction of the MET in each Z event is the template which corresponds to the njet and sum jet p_T in the Z event. The prediction for the Z sample is simply the sum of all such templates.

In both the case of QCD and photon templates, a variety of triggers with different p_T thresholds are need in order to properly sample the templates. Each of these triggers has a different prescale which varies over the course of data taking. It is therefore necessary to take this prescale into account when creating the templates so that the prediciton is not biased by the lower prescale triggers. This is done by applying a weight to the event when filling the templates. The weight is the product of L1 and HLT prescales. Each trigger used has a separate set of templates, which in effect means that the triggers are MET distributions binned in three dimensions: njet, sum jet p_T , and trigger.

10

Table 3: Data and Monte Carlo yields for the tight signal region MET > 200 GeV for 204 pb^{-1}.

Sample	ee	$\mu\mu$	$e\mu$	tot
Z+Jets	0.000 ± 0.000	0.000 ± 0.000	0.000 ± 0.000	0.000 ± 0.000
$t\bar{t}$	0.181 ± 0.074	0.181 ± 0.074	0.483 ± 0.121	0.845 ± 0.160
WJets	0.000 ± 0.000	0.000 ± 0.000	0.000 ± 0.000	0.000 ± 0.000
WW	0.000 ± 0.000	0.008 ± 0.008	0.008 ± 0.008	0.017 ± 0.012
WZ	0.025 ± 0.007	0.021 ± 0.006	0.000 ± 0.000	0.046 ± 0.009
ZZ	0.013 ± 0.003	0.013 ± 0.003	0.000 ± 0.000	0.026 ± 0.004
Single Top	0.000 ± 0.000	0.013 ± 0.008	0.009 ± 0.006	0.022 ± 0.010
LM4	0.922 ± 0.040	0.969 ± 0.041	0.128 ± 0.015	2.019 ± 0.060
LM8	0.345 ± 0.015	0.387 ± 0.016	0.144 ± 0.010	0.876 ± 0.024
Total MC	0.219 ± 0.074	0.237 ± 0.075	0.500 ± 0.121	0.956 ± 0.161
Data	0	2	2	4
LM4	0.922 ± 0.040	0.969 ± 0.041	0.128 ± 0.015	2.019 ± 0.060
LM8	0.345 ± 0.015	0.387 ± 0.016	0.144 ± 0.010	0.876 ± 0.024

Table 4: Details of data events for the loose signal region MET > 100GeV for 204 pb^{-1}. The SimpleSecondaryVertexTagger high efficiency medium working point is used for b-tagging.

Run	Lumi Section	Event	Lep Type	Njet	N B Tag	pfMET	tcMET	Dilep Mass	Sum jet p_T	Z p_T
161312	963	366557890	e	4	2	117.1	117.9	89.0	218.9	18.1
163069	432	236566401	e	2	1	107.4	92.3	83.6	213.9	90.9
163758	86	64208683	e	2	0	119.5	114.1	82.6	114.0	58.6
163758	63	46610542	e	4	0	124.1	41.4	91.1	300.1	261.9
163332	615	415350358	e	4	0	115.6	108.6	100.1	316.7	108.3
163332	730	489406176	e	2	0	100.4	88.4	92.6	98.6	52.8
163817	680	633297354	e	4	0	165.0	155.0	89.7	437.8	26.0
163659	320	243264615	μ	2	0	150.0	130.2	86.1	192.7	71.1
163663	181	126212285	μ	3	1	102.3	79.9	85.4	210.5	49.8
163584	54	39429230	μ	3	0	209.6	217.4	92.5	349.6	29.2
160873	115	30074254	μ	2	1	102.8	87.8	89.1	89.9	78.5
163255	673	435619707	μ	2	2	169.4	160.6	96.0	140.4	108.0
163759	80	52493009	μ	2	0	239.3	229.0	87.5	198.7	109.4
163233	8	3963812	μ	2	0	106.2	103.3	82.9	123.0	58.0

In order to avoid contamination of events with real MET from W bosons, events with leptons are vetoed when making templates.

While there is in principle a small contribution from $t\bar{t}$ in the Z sample from which we predict the MET distribution, it is only $\approx2.6\%$ of the total sample used (MC expectation), as shown in table 1, and the data driven prediction (see Fig. 8) estimates that the $t\bar{t}$ contribution to the loose signal region is $\approx0.3\%$ of the total Z yield. As the MET measurement in these events does not enter the MET prediction, this small non-Z contribution is negligible.

The above outlines the template method and was general to both QCD and photon samples. In the subsections below, we discuss the slightly different procedure which is necessary in deriving and applying the two sets of templates, and then compare the results obtained from each.

6.2 QCD Templates

The QCD sample is selected using single jet triggers which are listed in appendix A.3. The lead jet p_T in the QCD event determines which of the trigger bins the event enters according to the thresholds lised in appendix A.3. In order to make a reliable prediction, the same quantity with the same thresholds must be used to pick template is used to predict a Z event. Therefore the lead jet p_T in the Z sample is used

to pick the QCD template trigger bin.

The one significant difference between QCD and photon plus jets events is that in photon plus jets events, the jet system may recoil against the photon. Since the photon in general contributes less MET to the event than the jets, the recoil against the photon tends to increase the MET in photon plus jets events compared to QCD events with similar njet and sum jet pt.

To model this effect, a smearing procedure is applied to the QCD templates when making the prediction for the Z sample which depends on the p_T of the Z. We estimate the magnitude of this effect using the photon sample by plotting the dot product of the photon p_T and the MET divided by the photon p_T squared:

$$\frac{\overrightarrow{p_T}_{photon} \cdot \overrightarrow{MET}}{|\overrightarrow{p_T}_{photon}|^2} \tag{1}$$

The distribution of this quantity is peaked at 6% and is gaussian. It does not depend strongly on the number of jets nor the photon p_T. We therefore take 6% of the Z p_T when making this correction as the MET contribution from the boson recoil. Then for each bin in the template, this MET contributin is added and averaged over a number of different angles to obtain a new template which is used to make the final predicition from the QCD sample.

6.3   Photon Templates

The photon sample used to create the photon templates is obtained from the single photon triggers listed in appendix A.2. As in the QCD case, each trigger feeds its own set of templates (MET distributions binned in njet and sum jet pt). Each photon event enters the template for the highest p_T photon trigger which fired in the event.

In order to make the prediction of the MET in the Z sample, each Z event is assigned one unit area template based on its number of jets, the scalar sum of jet p_T and the Z p_T. The Z p_T enters only in choosing which bin of photon trigger to use. This is done because the Z p_T is the analogous variable in the Z sample to the photon p_T. The Z p_T ranges used for each trigger are shown in appendix A.2 and are chosen to take into account the turn-on of the photon trigger.

We show all the templates used in appendix B.

6.4   Comparison of QCD and Photon Template Predictions

The procedure and templates described above are applied to the Z sample passing the preselection described in section 4. In this section we do not show the Z data but instead focus on the two independent data driven predictions. The results including the Z data are given in section 10.

Figure 4 shows the two resulting MET predictions as well as their integrals.

The two predictions are found to be consistent with one another within their statistical and systematic uncertainties (systematic uncertainties on the template method are discussed in section 11.1). Therefore we see no need to derive two separate predictions and limits, so we pick the photon templates because the photon plus jet event topology is more similar to the Z plus jets event topology.

7   Closure Test of Templates in MC

The above procedure is applied to MC to test its effectiveness under 'ideal' conditions. In order to test the results obtained in section 6.4, we construct templates separately from PhotonJet MC and QCD MC. These templates are then used to predict the MET distribution in ZJets MC. The MC samples used are:

- PhotonJet MC

    - /G_Pt_15to30_TuneZ2_7TeV_pythia6/Spring11-PU_S1_START311_V1G1-v1/AODSIM
    - /G_Pt_30to50_TuneZ2_7TeV_pythia6/Spring11-PU_S1_START311_V1G1-v1/AODSIM

Dilepton data predicted from QCD; ee+μμ; njet >= 2

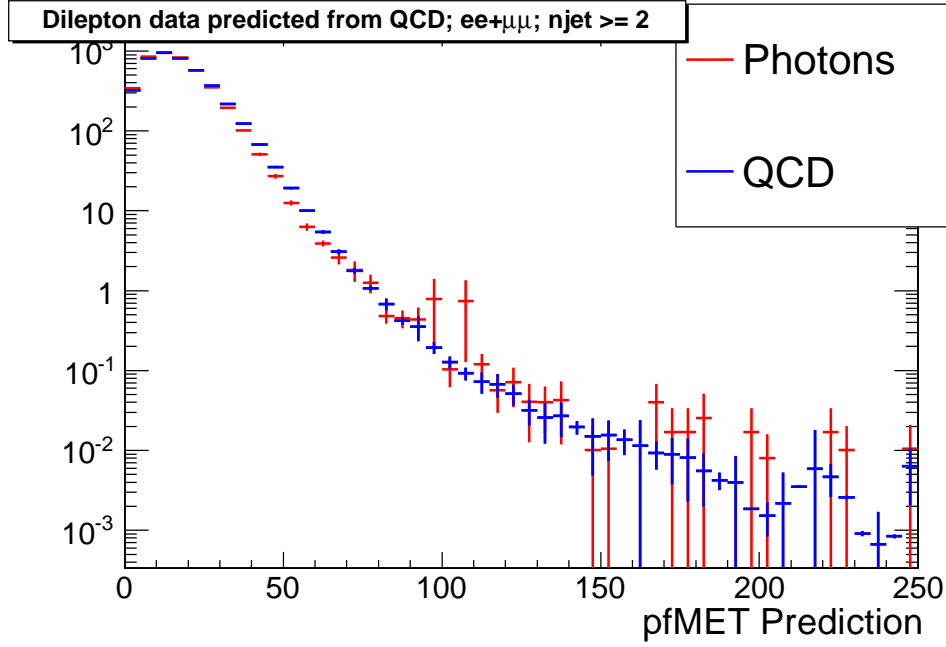| MET	> 30 GeV	> 60 GeV	> 100 GeV	> 200
photon	406.20 ± 7.10	13.13 ± 1.23	1.40 ± 0.62	0.05 ± 0.02
QCD	486.71 ± 4.88	13.66 ± 0.42	0.64 ± 0.06	0.03 ± 0.01

Figure 4: The predicted MET distribution from QCD templates (blue) and photon plus jets templates (red). Below the plot is tabulated the integral of each prediction for MET > 30 GeV, > 60 GeV, > 100 GeV, and > 200 GeV.

283   – /G_Pt_50to80_TuneZ2_7TeV_pythia6/Spring11-PU_S1_START311_V1G1-v1/AODSIM

284   – /G_Pt_80to120_TuneZ2_7TeV_pythia6/Spring11-PU_S1_START311_V1G1-v1/AODSIM

285   – /G_Pt_120to170_TuneZ2_7TeV_pythia6/Spring11-PU_S1_START311_V1G1-v1/AODSIM

286   – /G_Pt_170to300_TuneZ2_7TeV_pythia6/Spring11-PU_S1_START311_V1G1-v1/AODSIM

287 • QCD MC

288   – /QCD_Pt_15to30_TuneZ2_7TeV_pythia6/Spring11-PU_S1_START311_V1G1-v1/AODSIM

289   – /QCD_Pt_30to50_TuneZ2_7TeV_pythia6/Spring11-PU_S1_START311_V1G1-v1/AODSIM

290   – /QCD_Pt_50to80_TuneZ2_7TeV_pythia6/Spring11-PU_S1_START311_V1G1-v1/AODSIM

291   – /QCD_Pt_80to120_TuneZ2_7TeV_pythia6/Spring11-PU_S1_START311_V1G1-v1/AODSIM

292   – /QCD_Pt_120to170_TuneZ2_7TeV_pythia6/Spring11-PU_S1_START311_V1G1-v1/AODSIM

293   – /QCD_Pt_170to300_TuneZ2_7TeV_pythia6/Spring11-PU_S1_START311_V1G1-v1/AODSIM

294 • ZJet MC

295   – /DYToEE_M-20_CT10_TuneZ2_7TeV-powheg-pythia/Spring11-PU_S1_START311_V1G1-v1/AODSIM

296   – /DYToMuMu_M-20_CT10_TuneZ2_7TeV-powheg-pythia/Spring11-PU_S1_START311_V1G1-v1/AODSI

297   – /DYToTauTau_M-20_CT10_TuneZ2_7TeV-powheg-pythia-tauola/Spring11-PU_S1_START311_V1G1

298 Good agreement between the observed and predicted MET distributions is observed for each MC sample,

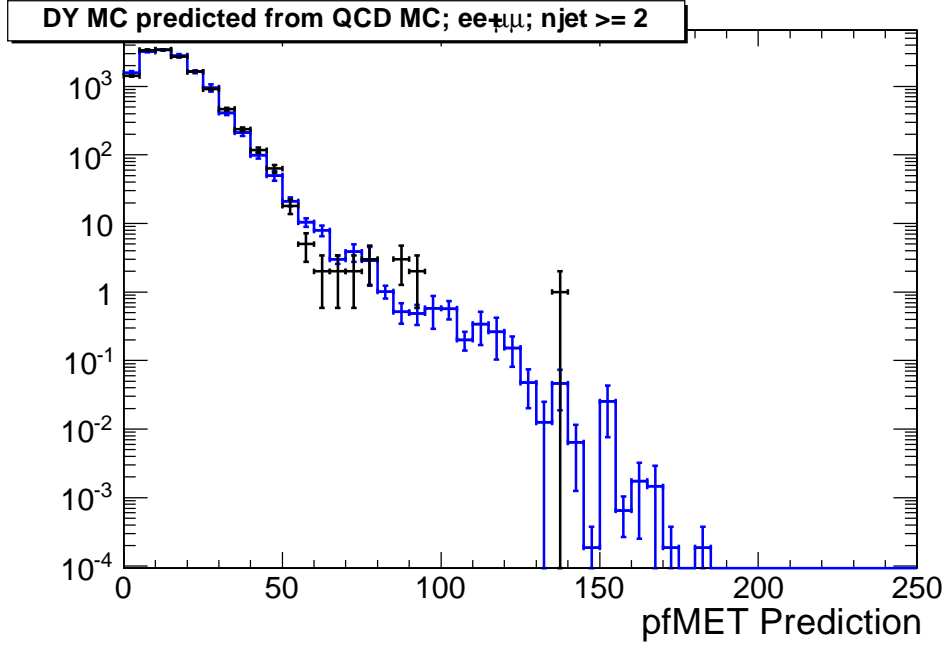299 as well as between the two samples, as shown in figures 6 and 5.

MET	> 30 GeV	> 60 GeV	> 100 GeV	> 200
Z MC	921	15	1	0
Prediction	824.20 ± 38.99	21.89 ± 2.52	1.67 ± 0.31	0.00 ± 0.00

Figure 5: The MET distribution in Z plus jets MC (black) and prediction (blue) for Njet ≥ 2. Below the plot is tabulated the integral of the Z plus jets MC MET and the predicted MET from QCD MC for MET > 30 GeV, > 60 GeV, > 100 GeV, and > 200 GeV.

8 Top Background Estimation

The MET templates method is used to estimate the contribution of SM Z production to the signal region due to the fake MET tail. However, it does not account for the $t\bar{t}$ background in which the dileptons happen to lie in the Z mass window, which is accompanied by genuine MET. To estimate this contribution we use an opposite-flavor subtraction technique which takes advantage of the fact that the $t\bar{t}$ yield in the opposite-flavor final state ($e\mu$) is the same as in the same-flavor final state ($ee+\mu\mu$), modulo differences in efficiency in the e vs. μ selection. Hence the $t\bar{t}$ yield in the same-flavor final state can be estimated using the corresponding yield in the opposite-flavor final state. It is important to note that other backgrounds for which the lepton flavors are uncorrelated (for example WW and DY$\to \tau\tau$) will also be included in this estimate.

The simplest option is to take the $e\mu$ yield inside the Z mass window and scale this to predict the ee and $\mu\mu$ yields, based on e and μ selection efficiencies. Only the ratio of muon to electron selection efficiency is needed, which we evaluate as $\epsilon_{\mu e} = \sqrt{\frac{N_{Z\mu\mu}}{N_{Zee}}}$. Here N_{Zee} ($N_{Z\mu\mu}$) is the total number of events in the ee ($\mu\mu$) final state passing the pre-selection in Section 4, without the requirement of at least 2 jets. We find $\epsilon_{\mu e} = 1.067 \pm 0.003$ (stat). (Note that in the following $\epsilon_{e\mu} = 1/\epsilon_{\mu e}$.) Systematic uncertainties on the prediction are assessed in section 11.2, and only statistical uncertainties are given in this section.

This procedure yields the following predicted yields n_{pred}, based on an observed yield of 12 $e\mu$ events in the loose signal region (the corresponding predictions in the tight signal region are shown in figures 9 and 10):

$$n_{pred}(\mu\mu) = \frac{1}{2}n(e\mu)\epsilon_{\mu e} = 6.40 \pm 1.85 \tag{2}$$

$$n_{pred}(ee) = \frac{1}{2}n(e\mu)\epsilon_{e\mu} = 5.62 \pm 1.62 \tag{3}$$

14

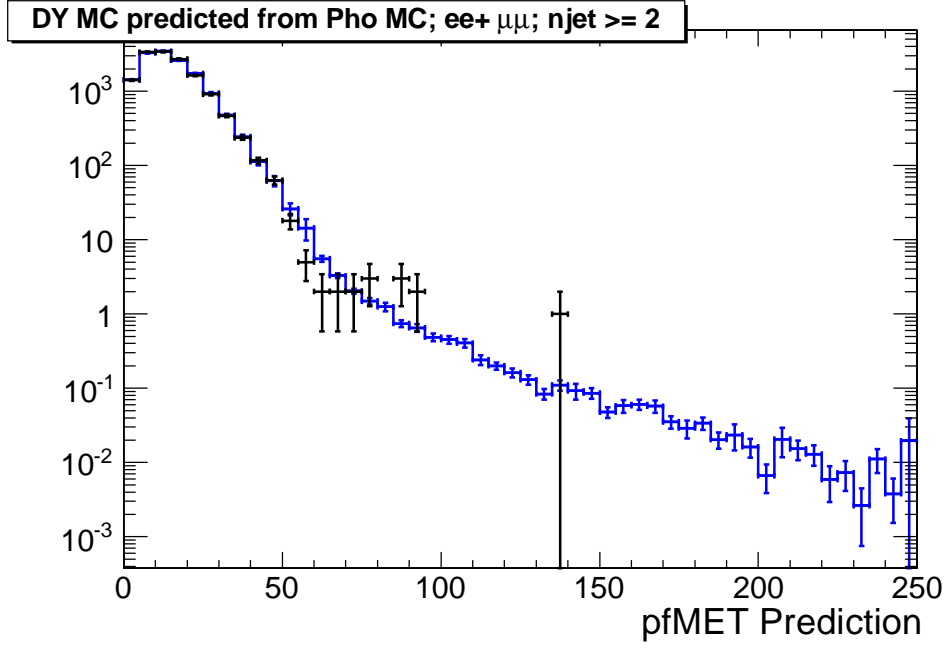| MET	> 30 GeV	> 60 GeV	> 100 GeV	> 200
Z MC	921	15	1	0
Prediction	959.15 ± 27.00	19.39 ± 0.58	2.28 ± 0.09	0.07 ± 0.01

Figure 6: The MET distribution in Z plus jets MC (black) and prediction (blue) for Njet $\geq$ 2. Below the plot is tabulated the integral of the Z plus jets MC MET and the predicted MET from photon plus jets MC for MET > 30 GeV, > 60 GeV, > 100 GeV, and > 200 GeV.

The predicted same flavor $t\bar{t}$ yields can be compared with the MC expectation of 4.3 ($\mu\mu$) and 3.7 (ee) as shown in Table 2. Due to the relatively small statistics, the errors on the predicted yields using this procedure are fairly large. To improve the statistical errors, we instead determine the $e\mu$ yield without requiring the leptons to fall in the Z mass window. This yield is scaled by a factor determined from MC, $K = 0.16$, which accounts for the fraction of $t\bar{t}$ events expected to fall in the Z mass window. This procedure yields the following predicted yields based on 74 observed $e\mu$ events:

$$n_{pred}(\mu\mu) = \frac{1}{2}n(e\mu)K\epsilon_{\mu e} = 6.26 \pm 0.73 \tag{4}$$

$$n_{pred}(ee) = \frac{1}{2}n(e\mu)K\epsilon_{e\mu} = 5.50 \pm 0.64 \tag{5}$$

Notice that the yields are consistent with those predicted without using K, but the relative statistical uncertainty is reduced by a factor of approximately 2. Since the total uncertainty is expected to be statistically-dominated, the second method yields a better prediction and we use this as our estimate of the $t\bar{t}$ background.

9 Non $t\bar{t}$ Backgrounds

Backgrounds from pair production of vector bosons and single top can be reliably estimated from Monte Carlo. They are negligible compared to $t\bar{t}$ as shown in Tables 2 and 3.

Backgrounds from fake leptons are negligible due to the requirement of two $p_T > 20$ GeV leptons in the Z mass window, accompanied by jets and large MET.
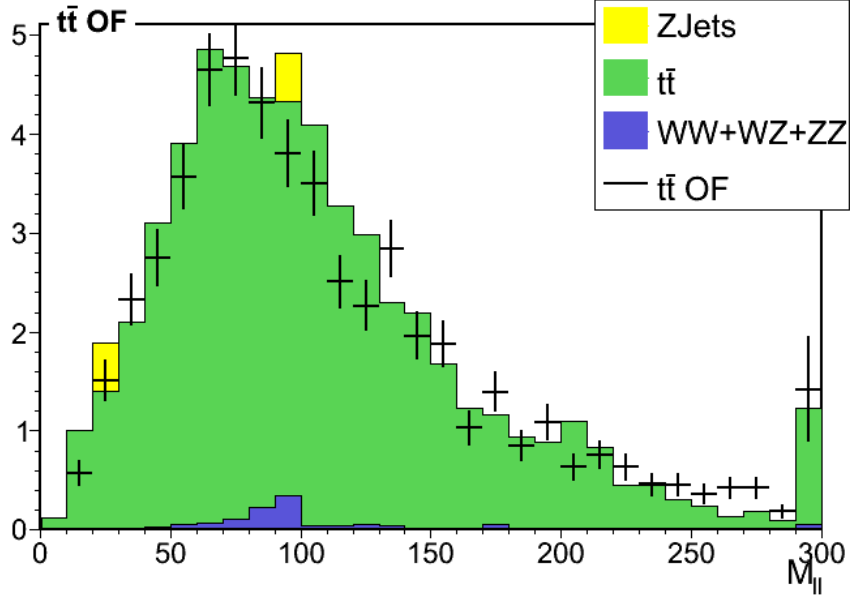
15

Figure 7: MC dilepton mass distribution for events passing the loose signal region selection. The solid histograms represent the yields in the same-flavor final state for each SM contribution, while the black data points (OFOS) indicates the sum of the $t\bar{t}$ MC contributions in the opposite-flavor final state. The $t\bar{t}$ distribution in the same-flavor final state is well-modeled by the OFOS prediction.

10   Results

The data and SM predictions are shown for all events in Fig. 8, and split between the ee and $\mu\mu$ final states in Fig. 9 and 10. We observe 14 events (7 in each lepton flavor channel) in the loose signal region (MET > 100GeV), compared to a data-driven prediction of 13.16 ± 1.15 which is dominated by the estimated $t\bar{t}$ contribution. For the tight signal region defined by MET > 200GeV, we observe 2 events (both in the $\mu\mu$ channel) compared to a data-driven prediction of 1.18 ± 0.33 (Recall from table 3 that there are two $e\mu$ events in the tight signal region.) The uncertainties quoted above are statistical only, and systematic uncertainties will be discussed in Sec. 11. We conclude that no excess of signal with respect to the data-driven prediciton is observed.

For display purposes only, in figures 8 through 10 we have taken the $t\bar{t}$ MET distribution from MC and normalized it such that the integral for MET>100 GeV matches the data-driven prediction from the OF subtraction.

11   Systematics Uncertainties in the Background Prediction

We discuss here the sources of uncertainty in the background predictions from the MET templates and OF subtraction methods.

11.1   Template Method Related Systematics

In this section, we list several sources of systematic uncertainties related to the template method, as summarized in table 5. We perform several variations in the template prediction and check the corresponding relative difference in the predicted yield for the control region of MET > 60. We have checked that the variations in the predicted yield do not depend strongly on the MET cut within statistical uncertainties. Therefore we use MET > 60 because the loose signal region (MET > 100) has large statistical uncertainty.

- A difference in Z p_T vs photon p_T introduces a difference in the boost of the hadronic system, which affects the MET distribution due to coherent mismeasurement of the hadronic activity. We test this using a reweighting procedure based on the distribution of the hadronic recoil p_T in the Z and

16
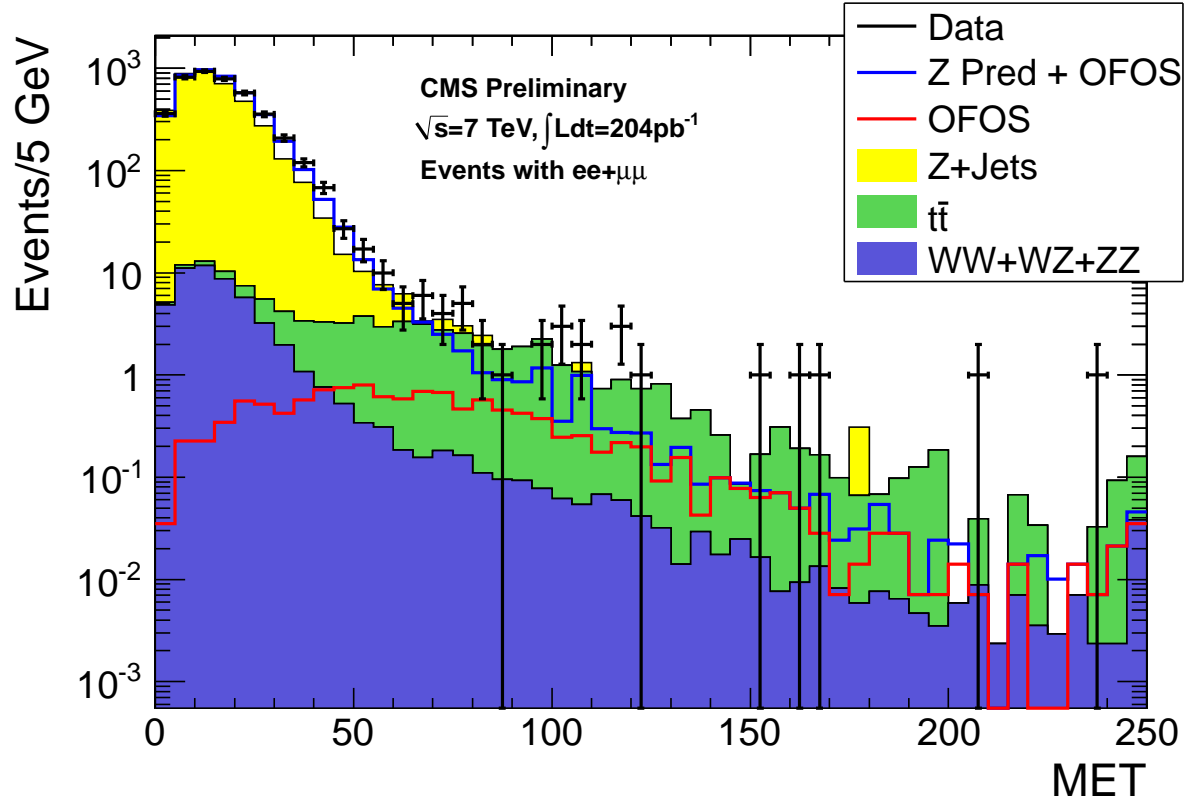
	MET > 30 GeV	MET > 60 GeV	MET > 100 GeV	MET > 200 GeV
Z pred	406.20 ± 7.10	13.13 ± 1.23	1.40 ± 0.62	0.05 ± 0.02
OFOS	54.77 ± 2.95	34.73 ± 2.35	11.76 ± 1.37	1.13 ± 0.46
Z pred + OFOS	460.97 ± 7.69	47.86 ± 2.66	13.16 ± 1.50	1.18 ± 0.46
Data	488	39	14	2

Figure 8: The observed MET distribution for data in the ee and $\mu\mu$ channels (black points), predicted $t\bar{t}$ MET distribution (red line), the sum of predicted $t\bar{t}$ MET distribution and Z MET distribution predicted from photon MET templates (solid blue line), and MC stacked for dominant backgrounds. Below the plot is tabulated the integral of the predicted MET distribution using the MET templates method (Z pred), the predicted ttbar yield using the opposite flavor subtraction technique (OFOS), the sum of these two contributions (Z pred + OFOS), and the observed MET distribution (data), for MET > 30 GeV and > 60 GeV (which are shown as cross checks), and for the signal regions of MET > 100 GeV and > 200 GeV.
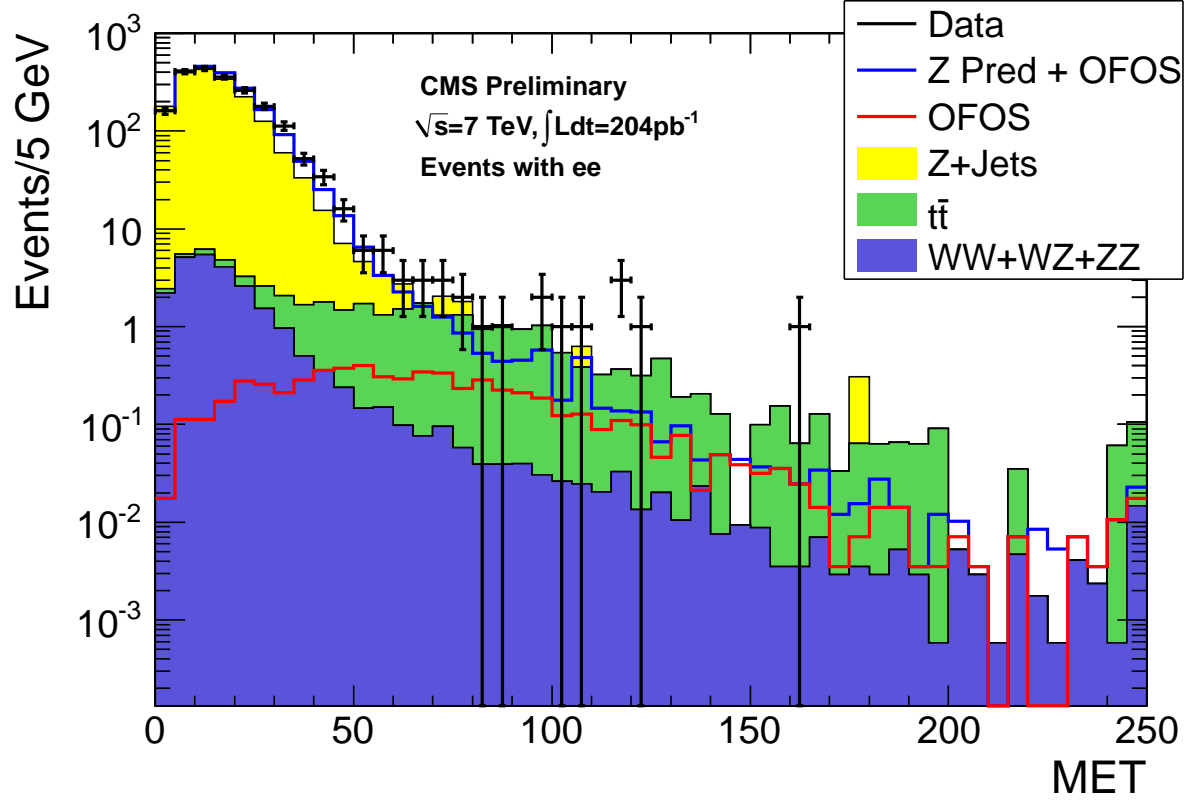
	MET > 30 GeV	MET > 60 GeV	MET > 100 GeV	MET > 200 GeV
Z pred	195.03 ± 3.39	6.58 ± 0.61	0.69 ± 0.30	0.02 ± 0.01
OFOS	25.60 ± 1.38	16.24 ± 1.10	5.50 ± 0.64	0.53 ± 0.22
Z pred + OFOS	220.64 ± 3.66	22.81 ± 1.26	6.19 ± 0.71	0.55 ± 0.22
Data	249	22	7	0

Figure 9: The observed MET distribution for data in the ee channels (black points), predicted $t\bar{t}$ MET distribution (red line), the sum of predicted $t\bar{t}$ MET distribution and Z MET distribution predicted from photon MET templates (solid blue line), and MC stacked for dominant backgrounds. Below the plot is tabulated the integral of the predicted MET distribution using the MET templates method (Z pred), the predicted ttbar yield using the opposite flavor subtraction technique (OFOS), the sum of these two contributions (Z pred + OFOS), and the observed MET distribution (data), for MET > 30 GeV and > 60 GeV (which are shown as cross checks), and for the signal regions of MET > 100 GeV and > 200 GeV.
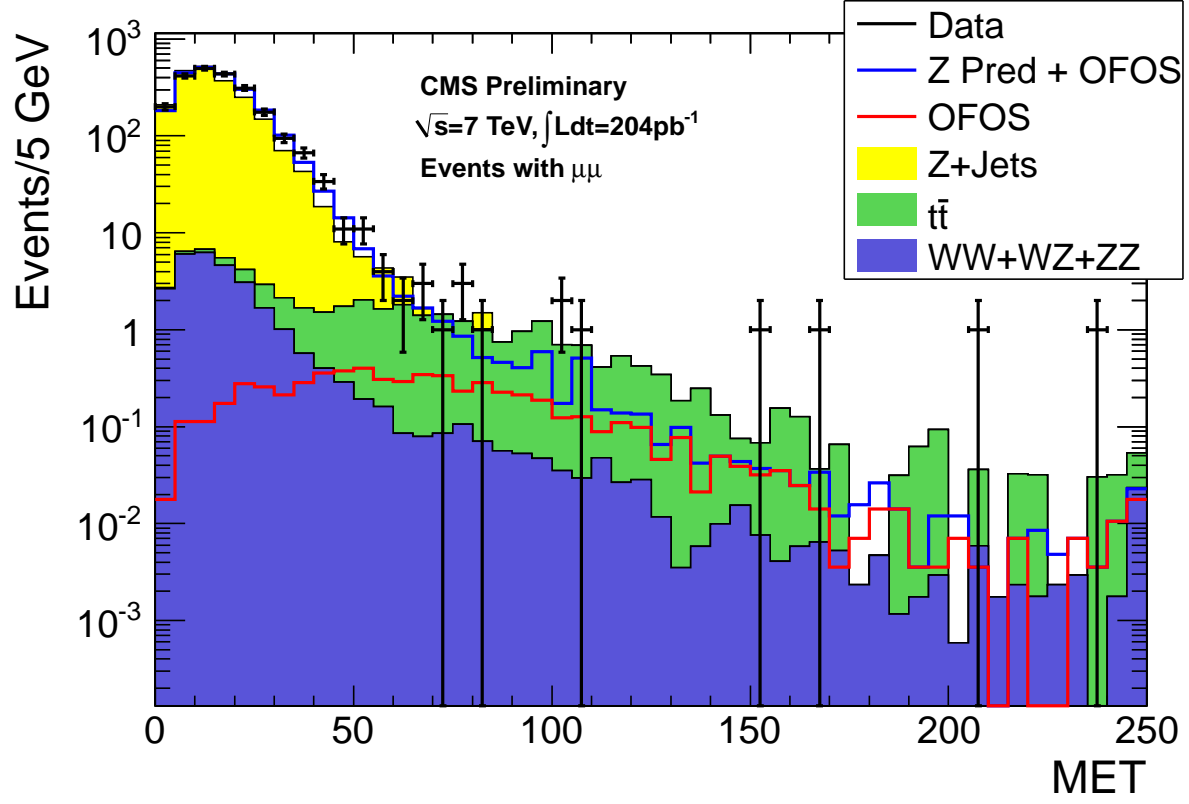
	MET > 30 GeV	MET > 60 GeV	MET > 100 GeV	MET > 200 GeV
Z pred	211.17 ± 3.74	6.55 ± 0.63	0.71 ± 0.32	0.02 ± 0.01
OFOS	29.16 ± 1.57	18.49 ± 1.25	6.26 ± 0.73	0.60 ± 0.25
Z pred + OFOS	240.33 ± 4.06	25.04 ± 1.40	6.97 ± 0.79	0.63 ± 0.25
Data	239	17	7	2

Figure 10: The observed MET distribution for data in the $\mu\mu$ channels (black points), predicted $t\bar{t}$ MET distribution (red line), the sum of predicted $t\bar{t}$ MET distribution and Z MET distribution predicted from photon MET templates (solid blue line), and MC stacked for dominant backgrounds. Below the plot is tabulated the integral of the predicted MET distribution using the MET templates method (Z pred), the predicted ttbar yield using the opposite flavor subtraction technique (OFOS), the sum of these two contributions (Z pred + OFOS), and the observed MET distribution (data), for MET > 30 GeV and > 60 GeV (which are shown as cross checks), and for the signal regions of MET > 100 GeV and > 200 GeV.

Table 5: Summary of variations in the MET templates prediction. The yields predicted by the MET templates method in the control region of MET> 60 GeV are shown, along with the relative difference with respect to the nominal prediction for several sources of variation in the template prediction.

	N(MET> 60 GeV)	Rel Diff
Nominal	13.13 ± 1.23	
vary photon selection (h/e < 0.05)	13.14 ± 1.28	-0.00
vary photon selection (h/e < 0.01)	11.72 ± 1.03	0.11
vary photon selection (emf > 0.8)	12.18 ± 1.18	0.07
vary photon selection (emf > 0.9)	11.11 ± 0.88	0.15
hadronic recoil P_T reweighting	15.76 ± 1.08	-0.20
nVtx reweighting	13.02 ± 1.16	0.01

photon samples. We normalize to unit area the distributions of hadronic recoil p_T in the 2 samples, and assess to each photon event a weight which is equal to the ratio of the Z p_T contributions in the corresponding bin of hadronic recoil p_T . This procedure gives a relative difference of 20% in the predicted yield and we assess a corresponding uncertainty.

- The photon triggers are prescaled as the instantaneous luminosity increased. As a result, the number of pile up events is different in Z events than in photon events, as the latter were preferentially taken at lower instantaneous luminosity. However, this difference is largely compensated because the photon events are weighted by the trigger rescale. We perform the same reweighting procedure using the nVertex distribution in Z and photon events. This procedure gives uncertainties of approximately 1%, which we regard as negligible.

- Backgrounds to the photon sample from events where the "photon object" includes hadronic energy that was lost will artificially increase the MET templates. If this was a significant effect, then altering the photon selection ought to significantly change the MET prediction. We test for this by by tightening the cuts on neutral EM fraction and h/e. Based on these studies we assess an uncertainty of 15%.

Based on these studies we assess an uncertainty of 25% on the MET templates background prediction which is dominated by the difference in the Z vs. photon hadronic recoil p_T distributions. The resulting predictions with their statistical and systematic uncertainties for the $ee + \mu\mu$ final states are shown in table 6.

Table 6: Results of assessing 25% systematics to the MET template prediction shown in figure 8.

	MET > 30 GeV	MET > 60 GeV	MET > 100 GeV	MET > 200 GeV
Z Pred	$406.20 \pm 7.10 \pm 101.55$	$13.13 \pm 1.23 \pm 3.28$	$1.40 \pm 0.62 \pm 0.35$	$0.05 \pm 0.02 \pm 0.01$

11.2 Systematics of OF Subtraction

The uncertainty on the background prediction from the OF subtraction (see section 8) comes from the uncertainties in 2 quantities: $\epsilon_{e\mu} = \epsilon(e)/\epsilon(\mu)$, the ratio of muon to electron selection efficiencies, and K, the fraction of $t\bar{t}$ events which fall inside the Z mass window. The value of $\epsilon_{e\mu} = \epsilon(e)/\epsilon(\mu)$ is found to be ≈ 1.06, so we take as a systematic half of the difference to unity, or 3%. The uncertainty in K is due to the uncertainty in the lepton energy scale and is therefore quite small. Varying the boundaries of the Z mass window by ± 2 GeV results in a relative change in K of 2% and we assess a corresponding uncertainty. The total systematic undertainty is therefore 3.6% .

Based on these studies we find the predicted $t\bar{t}$ yields from the OF subtraction technique as shown in table 7.

Table 7: Results of assessing 3.6% systematics to the OF prediction shown in figure 8.

	MET > 30 GeV	MET > 60 GeV	MET > 100 GeV	MET > 200 GeV
OFOS Pred	$54.77 \pm 2.95 \pm 1.97$	$34.73 \pm 2.35 \pm 1.25$	$11.76 \pm 1.37 \pm 0.42$	$1.13 \pm 0.46 \pm 0.04$

12 Upper Limit on Non SM Yield

The results of summing the predicted backgrounds from the MET templates and OF subtraction methods are shown in table 8.

Table 8: Combination of predictions from MET templates and OF subtraction.

	MET > 30 GeV	MET > 60 GeV	MET > 100 GeV	MET > 200 GeV
Prediction	$460.97 \pm 7.69 \pm 101.57$	$47.86 \pm 2.66 \pm 3.51$	$13.16 \pm 1.50 \pm 0.55$	$1.18 \pm 0.46 \pm 0.04$

Using the results of the background predictions shown in table 8, we calculate the Bayesian 95% CL upper limits on the non SM event yields (Gaussian nuissance parameter model) shown in table 9.

Table 9: Model independent upper limit (UL) on non-SM event yields.

	MET > 30 GeV	MET > 60 GeV	MET > 100 GeV	MET > 200 GeV
Prediction	460.97 ± 101.86	47.86 ± 4.40	13.16 ± 1.60	1.18 ± 0.46
Data	488	39	14	2
UL	224.85	11.95	10.22	5.38

13 Additional Information for Model Testing

Other models of new physics in the dilepton final state can be confronted in an approximate way by simple generator-level studies that compare the expected number of events in 34.0 pb^{-1} with our upper limits of 7.9 events (loose signal region) and 3.0 events (tight signal regions). The key ingredients of such studies are the kinematic cuts described in this note, the lepton efficiencies, and the detector response for MET.

The muon identification efficiency is $\approx 92\%$; the electron identification efficiency varies from $\approx 86\%$ at $P_T = 20$ GeV to 93% for $P_T > 50$ GeV (see Fig. 11 top).

The lepton isolation efficiency varies with lepton momentum, as well as the jet activity in the event. In $t\bar{t}$ events, it varies from $\approx 87\%$ (muons) and $\approx 90\%$ (electrons) at $P_T = 20$ GeV to $\approx 95\%$ for $P_T > 60$ GeV. In LM4 (LM8) events, this efficiency is degraded by $\approx 2 - 5\%$ ($\approx 10 - 13\%$) over the whole momentum spectrum (see Fig. 11 bottom).

The average detector response (the reconstructed quantity normalized to the generated quantity) for MET is $0.96 \pm X$ where the uncertainties originate from the hadronic energy scale uncertainty. The experimental resolution on this quantity is 17%.

14 Model-Dependent Limits

As an example of how the upper limit presented in Sec. 12 can be used to test if a specific model is excluded, in this section we consider the benchmark SUSY processes LM4 and LM8, which contain Z bosons produced in the cascade decays of SUSY particles. We place upper limits on the quantity $\sigma \times BF \times A$, assuming efficiencies and uncertainties from these processes, and compare them to the expected values of $\sigma \times BF \times A$. Here σ is the signal production cross section, BF is the branching fraction to the final state Z + jets + MET and A is the signal acceptance.

The signal event yield N_{SIG} can be expressed as:

$$N_{SIG} = \sigma \times BF \times A \times \epsilon \times \mathcal{L}, \tag{6}$$

and we therefore have:

$$N_{SIG}/(\epsilon \times \mathcal{L}) = \sigma \times BF \times A. \tag{7}$$

Here ϵ is the signal efficiency and $\mathcal{L}$ is the integrated luminosity. Since we wish to place an upper limit on the quantity $\sigma \times BF \times A$, we must evaluate the quantity $N_{SIG}/(\epsilon \times \mathcal{L})$. Because of the efficiency in the denominator, this upper limit cannot be calculated in an entirely model-independent way; rather, it must be calculated with respect to a specific model. We therefore evaluate the upper limit on $\sigma \times BF \times A$ with respect to $t\bar{t}$, LM4 and LM8. For each process, we must calculate both the efficiency and its uncertainty, as discussed in the following subsections.

14.1 Signal Efficiencies

We evaluate the signal efficiencies using MC. To evaluate these efficiencies for our sample processes, we take as our denominator the number of generated events which pass the following selection at the generator level:

- 2 electrons or muons with $p_T > 20$ GeV and $|\eta| < 2.5$,

- Opposite-sign, same-flavor pair with $81 < M(ll) < 101$ GeV,

- Count genjets with $p_T > 30$ GeV, $|\eta| < 2.5$, $\Delta R > 0.4$ from any selected lepton as defined above,

- At least 2 genjets.

For the loose (tight) signal region efficiency, we add to this the requirement genmet> 60 (120) GeV. We take as our numerator the number of events passing the above generator-level selection which also pass the signal region selection at reco-level. For the loose (tight) signal region we find efficiencies of 43% (42%), 54% (55%)and 45% (48%) for $t\bar{t}$, LM4 and LM8, respectively. This efficiency is dominated by the dilepton selection efficiency, which varies from $\sim 0.6 - 0.7$ for the chosen processes.

14.2 Signal Efficiency Uncertainties

Here we assess systematic uncertainties in the signal efficiencies for our sample processes, from jet/MET, lepton identification, and luminosity uncertainties.

- Jets and MET selection efficiency: we assess this uncertainty by varying the hadronic energy scale by $\pm 5\%$ following the procedure used in the ttdilepton cross-section measurement. For the loose (tight) signal regions we find uncertainties of 9% (23%), 2% (4%), and 2%(4%) for $t\bar{t}$, LM4 and LM8, respectively.

- Lepton ID and isolation efficiencies: we perform a tag-and-probe technique on Z data and MC and find that the simulation agrees with data within about 2% as shown in Table 10. We apply a conservative 5% uncertainty on the dilepton selection efficiency.

- Trigger efficiency: the trigger efficiency is very close to 1 since there are 2 leptons with $p_T > 20$ GeV. We apply the simplified model of the trigger efficiency documented in [1] and assess the uncertainty as the relative difference in the yields between assuming 100% trigger efficiency vs. using the trigger model. This procedure gives differences of less than 1% and the trigger efficiency uncertainty is therefore regarded as negligible.

- Luminosity: we assess an uncertainty of 11%.

Table 10: Tag and probe results on $Z \to \ell\ell$ on data and MC. We quote ID efficiency given isolation and the isolation efficiency given ID.

	Data T&P	MC T&P
$\epsilon(id|iso)$ els	0.918 ± 0.003	0.936 ± 0.0038
$\epsilon(iso|id)$ els	0.986 ± 0.001	0.987 ± 0.0018
$\epsilon(id|iso)$ mus	0.962 ± 0.002	0.964 ± 0.0027
$\epsilon(iso|id)$ mus	0.987 ± 0.001	0.984 ± 0.0018

14.3 Upper Limits on $\sigma \times BF \times A$

Armed with the efficiencies and uncertainties calculated in the previous 2 sections, we proceed to calculate upper limits on the quantity $\sigma \times BF \times A$. We calculate Bayesian 95% CL upper limits using the cl95cms software, assuming a log-normal model of nuissance parameter integration. We also calculate the quantity $\sigma \times BF \times A$ for LM4 and LM8, for which we assume LO cross-sections of 1.88 pb and 0.73 pb and calculate k-factors for each event, depending on the sub-process. The quantity $BF \times A$ is taken to be the fraction of the total number of generated events which pass the generator-level selection given in Sec. 14.1. The results are summarized in Table 11. These results show that the LM4 and LM8 benchmark points are beyond the sensitivity of this search with the current integrated luminosity.

Table 11: Summary of efficiencies, efficiency uncertainties (quadrature sum of jet/MET, dilepton and luminosity uncertainties), and upper limits on $\sigma \times BF \times A$ for the loose (MET> 60 GeV) and tight (MET> 120 GeV) signal regions. We also show the quantity $\sigma \times BF \times A$ for LM4 and LM8.

	$t\bar{t}$	LM4	LM8
Loose signal region			
Efficiency	0.43	0.54	0.45
Efficiency Uncertainty	0.15	0.12	0.12
UL($\sigma \times BF \times A$) (pb)	0.56	0.44	0.53
$\sigma \times BF \times A$ (pb)		0.045	0.025
Tight signal region			
Efficiency	0.42	0.55	0.48
Efficiency Uncertainty	0.26	0.13	0.13
UL($\sigma \times BF \times A$) (pb)	0.23	0.17	0.19
$\sigma \times BF \times A$ (pb)		0.035	0.018

15 Conclusion

We have performed a search for BSM physics in the Z + jets + MET final state. Backgrounds from SM Z production were estimated using the data-driven MET templates method, and backgrounds from $t\bar{t}$ were estimated using the data-driven opposite-flavor subtraction technique. We found no evidence for anomalous yield beyond SM expectations and placed Bayesian 95% CL upper limits on the non SM yields in the loose (MET>60 GeV) and tight signal regions (MET>120 GeV), of 7.9 and 3.0 events, respectively. We also quoted upper limits on the quantity $\sigma \times BF \times A$, assuming efficiencies and uncertainties from the benchmark SUSY processes LM4 and LM8.
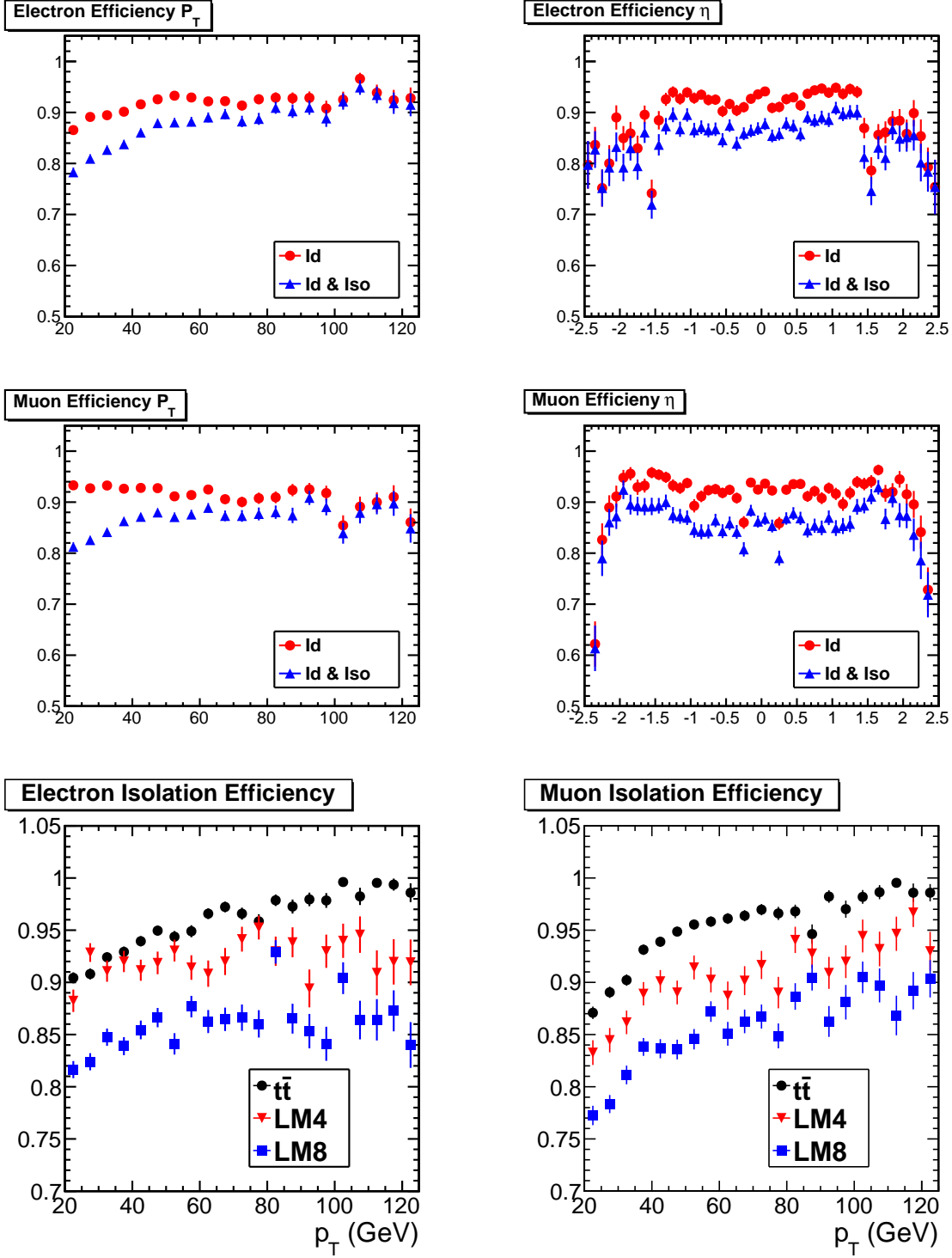
Figure 11: Identification and isolation efficiencies for leptons from $t \to W \to \ell$ and $t \to W \to \tau \to \ell$ in $t\bar{t}$ events (top). Isolation efficiency for $t\bar{t}$, LM4 and LM8 (bottom).
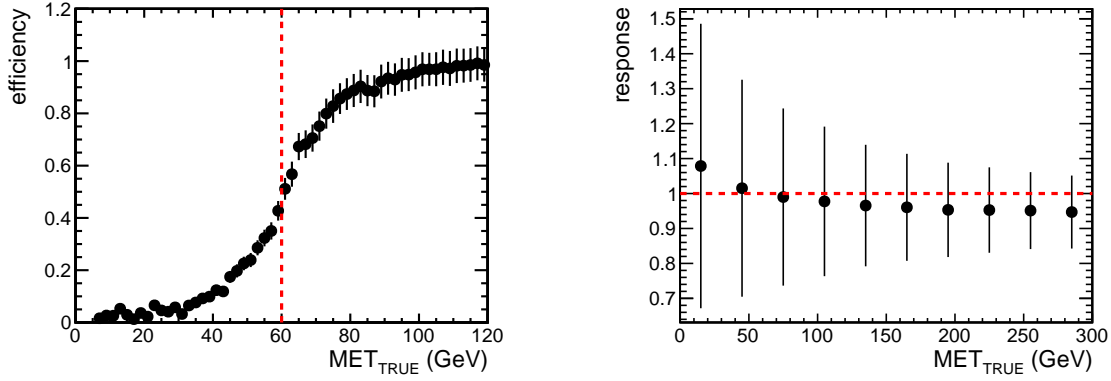
Figure 12: Left: the efficiency to pass the MET > 60 GeV requirement (indicated by the vertical dashed line) as a function of the true MET. Right: the average detector response (reconstructed MET divided by true MET) and its RMS, as a function of true MET. These plots are made with LM4 MC, but they are not expected to depend strongly on the underlying physics.

References

[1] arXiv:1103.1348v1, [2011 note]

[2] V. Pavlunin, Phys. Rev. **D81**, 035005 (2010).

[3] V. Pavlunin, CMS AN-2009/125

[4] A reference to the top paper, once it is submitted. Also D. Barge *et al.*, AN-CMS2010/258.

[5] Changes to the selection for the 38x CMSSW release are given in
https://twiki.cern.ch/twiki/bin/viewauth/CMS/TopDileptonRefAnalysis2010Pass5.

[6] https://twiki.cern.ch/twiki/bin/viewauth/CMS/SimpleCutBasedEleID

[7] https://twiki.cern.ch/twiki/bin/viewauth/CMS/EgammaWorkingPointsv3

[8] D. Barge *at al.*, AN-CMS2009/159.

[9] B. Mangano *et al.*, AN-CMS2010/283.

[10] https://twiki.cern.ch/twiki/bin/viewauth/CMS/CrossSections_3XSeries,
https://twiki.cern.ch/twiki/bin/view/CMS/ProductionSpring2011

[11] D. Barge *at al.*, AN-CMS2009/130.

[12] W. Andrews *et al.*, AN-CMS2009/023.

[13] D. Barge *at al.*, AN-CMS2010/257.

A Triggers

When listing triggers in this section, the version number is omitted for simplicity.

A.1 Dilepton Triggers

The triggers used for selecting dilepton events are:

- double-muon triggers
  - `HLT_DoubleMu7_v`
  - `HLT_Mu13_Mu7_v`
- double-electron triggers
  - `HLT_Ele17_CaloIdL_CaloIsoVL_Ele8_CaloIdL_CaloIsoVL_v`
  - `HLT_Ele17_CaloIdT_TrkIdVL_CaloIsoVL_TrkIsoVL_Ele8_CaloIdT_TrkIdVL_CaloIsoVL_TrkIsoV`
- e-μ cross triggers
  - `HLT_Mu17_Ele8_CaloIdL_v`
  - `HLT_Mu8_Ele17_CaloIdL_v`

A.2 Photon Triggers

The photon triggers used are:

- `HLT_Photon20_CaloIdVL_IsoL_v` ($Z\ p_T < 33$ GeV)

- `HLT_Photon30_CaloIdVL_IsoL_v` (33 GeV $< Z\ p_T < 55$ GeV)

- `HLT_Photon50_CaloIdVL_IsoL_v` (55 GeV $< Z\ p_T < 81$ GeV)

- `HLT_Photon75_CaloIdVL_IsoL_v` ($Z\ p_T > 81$ GeV)

The HLT requirements on the above triggers are [7]:

- CaloIdVL:
  H/E < 0.15 (0.1), $\sigma_{i\eta i\eta} < 0.024$ (0.04) in barrel (endcap)

- IsoL:
  Ecal ET $< 5.5 + 0.012$*ET, Hcal ET $< 3.5 + 0.005$*ET, Trk PT $< 3.5 + 0.002$*ET

A.3 Jet Triggers

The single jet triggers used to select the QCD sample from which the QCD MET templates are derived are listed below along with the thresholds applied to the lead jet pt for each trigger:

- `HLT_Jet30_v` ($p_T > 0$)

- `HLT_Jet60_v` ($p_T > 70$)

- `HLT_Jet80_v` ($p_T > 90$)

- `HLT_Jet110_v` ($p_T > 130$)

B MET Templates from Photon Sample

In this appendix we display our templates derived from the photon sample using the HLTPhoton20 (Fig. 13), HLTPhoton30 (Fig. 14), HLTPhoton50 (Fig. 15) and HLTPhoton70 (Fig. 16) triggers.
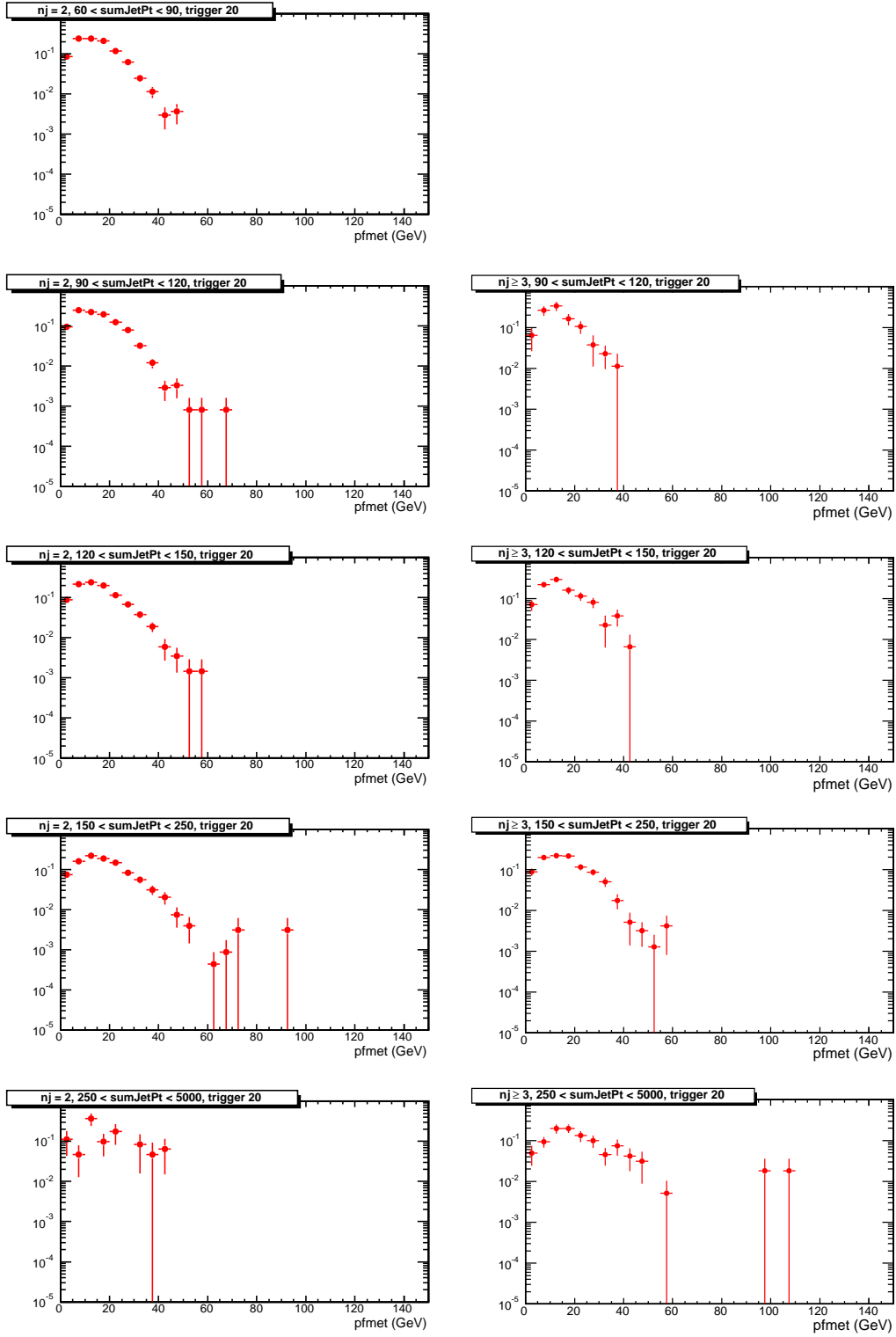
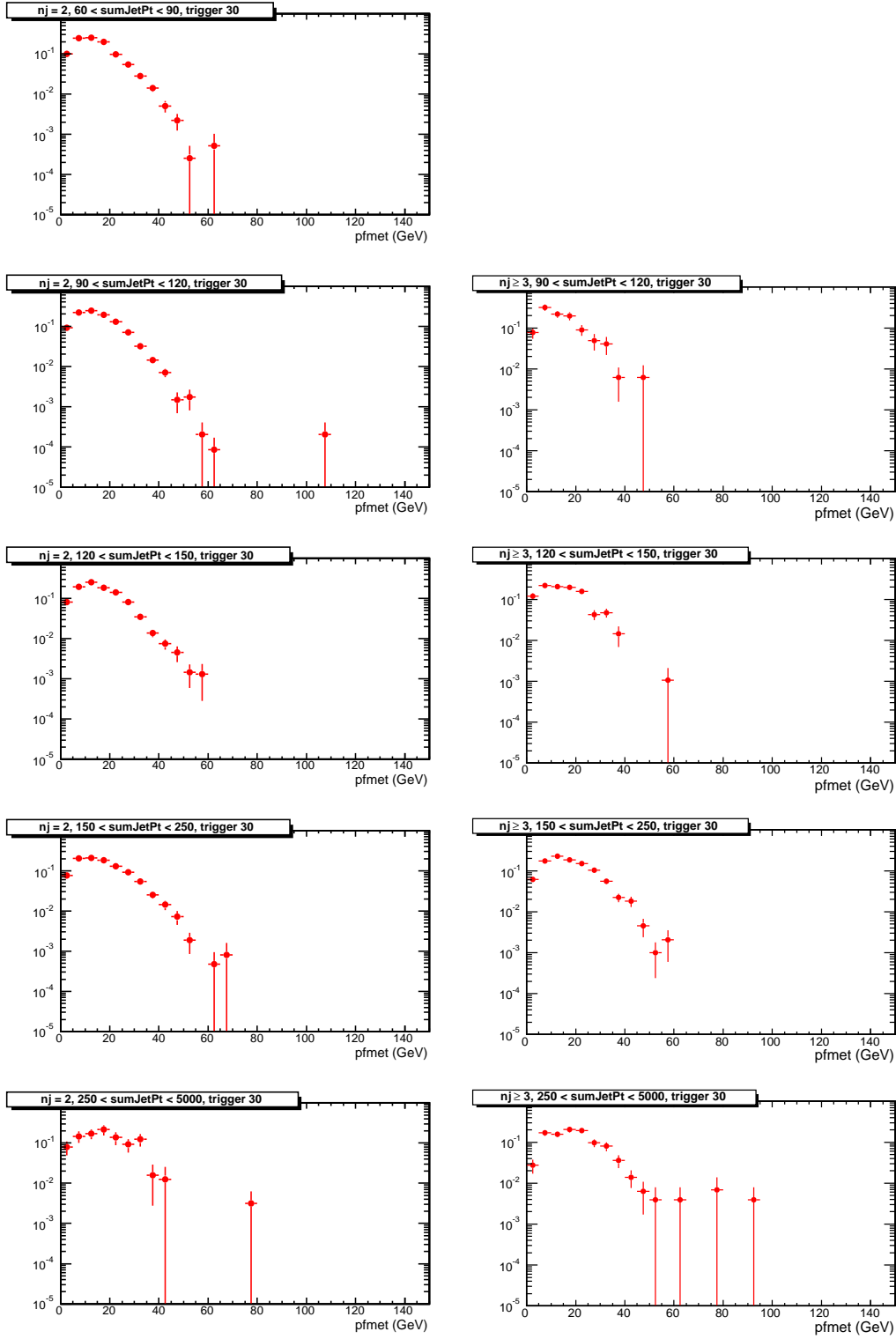Figure 13: MET Templates derived from the HLTPhoton20 sample.

Figure 14: MET Templates derived from the HLTPhoton30 sample.
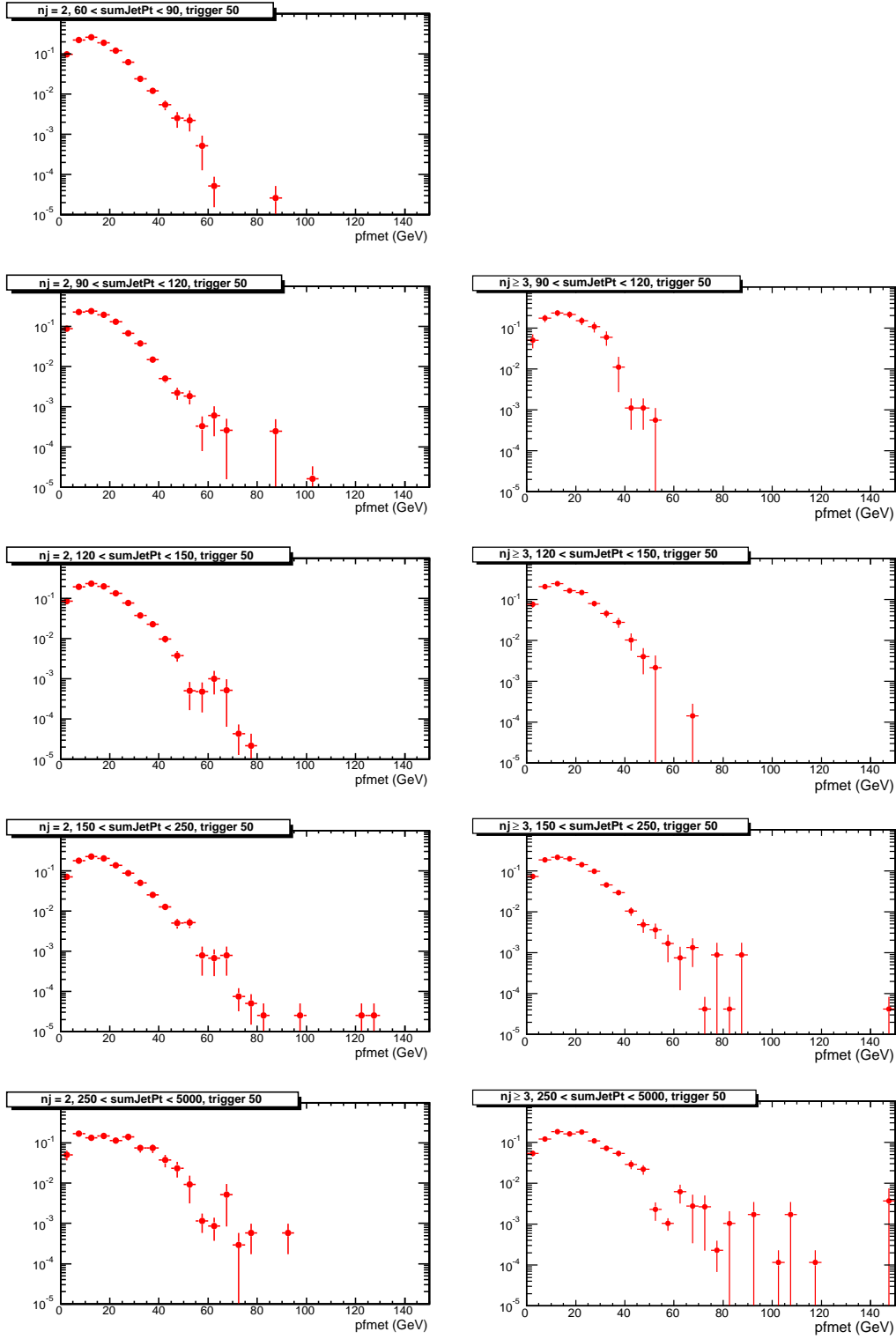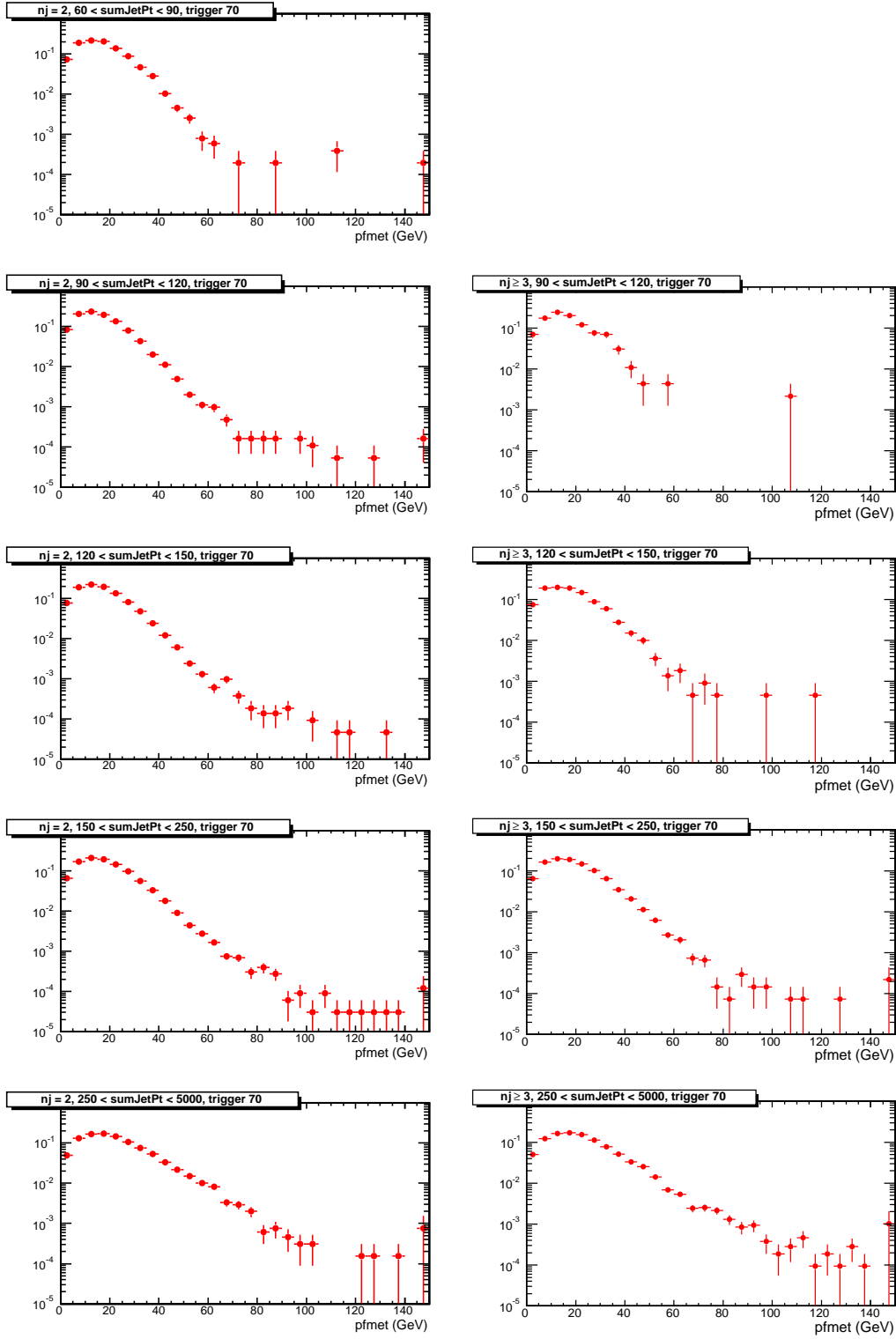
Figure 15: MET Templates derived from the HLTPhoton50 sample.

Figure 16: MET Templates derived from the HLTPhoton75 sample.